Support Information

Low Power High Purity Red Upconversion Emission and Multiple Temperature Sensing Behaviors in Yb^{3+},Er^{3+} codoped Gd_2O_3 Porous Nanorods

Wei Zheng, Baoyu Sun, Yuemei Li, Tiyi Lei, Rui Wang *, Jinzhu Wu**

School of Chemistry and Chemical Engineering, Harbin Institute of Technology, No. 92 Xidazhi Street, Nangang District, Harbin, Heilongjiang 150001, China

*Corresponding author:
Rui Wang *: *E-mail: wangrui001@hit.edu.cn;*
**Corresponding author:
Jinzhu Wu**: *E-mail: wujinzhu@hit.edu.cn*

Number of pages: 7
Number of Figures: 9
Number of Tables: 1

Experimental Section

Chemicals: $Er(NO_3)_3·5H_2O$ (99.9%), $Yb(NO_3)_3·5H_2O$ (99.9%), $Gd(NO_3)_3·6H_2O$(99.9%) and urea were purchased from Sigma-Aldric used without further purification. Deionized water as solvent was used throughout the experiment procedure.

Materials synthesis: First, $Gd(NO_3)_3·6H_2O$ (1.78 mmol), $Yb(NO_3)_3·5H_2O$ (0.2 mmol) and $Er(NO_3)_3·5H_2O$ (0.02 mmol) were completely dissolved in distilled water (10 mL) with constant stirring for 10 min. Then a certain amount of urea was added to the transparent solution, and the mixture was stirred at room for a period. Then, the resultant white precipitate was transferred to a Teflon autoclave and kept 453 K (24 h), leading to the formation of white precipitates. After that, the white precipitates washed by ethanol and water with centrifugation at 3000 $r·min^{-1}$ six times and dried in air at 333 K. Finally, the product was annealed under air atmosphere at 1073 K for 4 h to form $Gd_2O_3:Yb^{3+},Er^{3+}$ nanorods.

Materials Characterization: The morphologies and microstructures of all samples were investigated by SEM (SU8000), and TEM and HRTEM (JEOL, JEM-2100). The crystalline phases, composition and surface chemistry of samples were tested by XRD (Rigaku D/max-RB12 X-ray diffractometer with Cu Kα radiation). The thermogravimetry (TG) measurement was performed on a TA SDTQ600 instrument between 293 K and 1173 K with a heating rate of 5 K min^{-1}. The UV-visible absorption spectra spectrometer was tested by a Shimadzu and SPECORD S600 spectrophotometer. Upconversion PL spectra were recorded using by Zolix-SBP300 grating spectrometer equipped with CR131 photomultiplier tube. The 980 nm diode laser was used as pump source, and a signal generator was used to convert a continuous 980 nm excitation source to a pulse excitation source.

NIR laser treatment: The laser treatment was performed with a 980 nm InGaAs diode laser. The laser was fixed and irradiated at a power 1.51W. The white powder samples were pressed into pellets to laser irradiation treatment. To obtain laser treatment samples, the pellets samples were irradiated by 980 nm laser for 30 s.

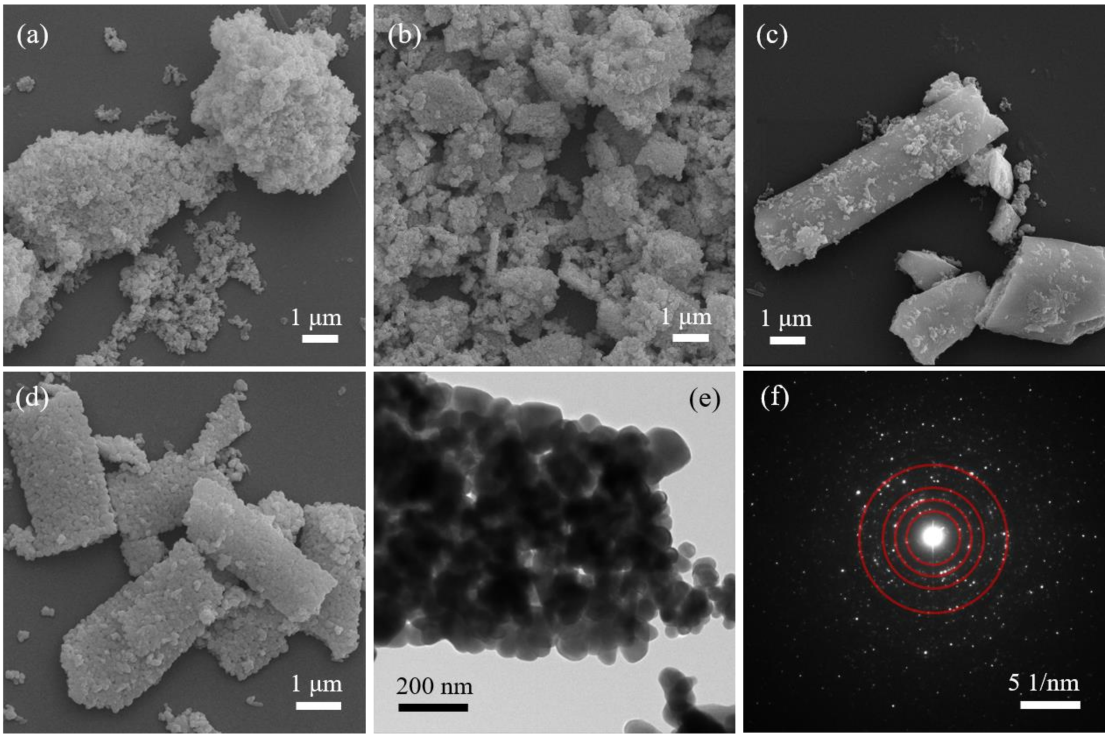

Figure S1. SEM image of the Gd_2O_3:10mol% Yb^{3+},1mol% Er^{3+} particles with different urea/Ln^{3+} ratio (a) urea/Ln^{3+} ratio: 1:1, (b) urea/Ln^{3+} ratio: 2:1. (c) SEM image of the $Gd_2O(CO_3)_2\cdot H_2O$:Yb^{3+},Er^{3+} particles (urea/Ln^{3+} ratio: 3:1). (d) SEM image of the Gd_2O_3:10mol% Yb^{3+},1mol% Er^{3+} particles (urea/Ln^{3+} ratio: 3:1). TEM image of the Gd_2O_3:10mol% Yb^{3+},1mol% Er^{3+} particles (urea/Ln^{3+} ratio: 3:1). (e) High resolution lattice image and (f) corresponding SAED pattern.

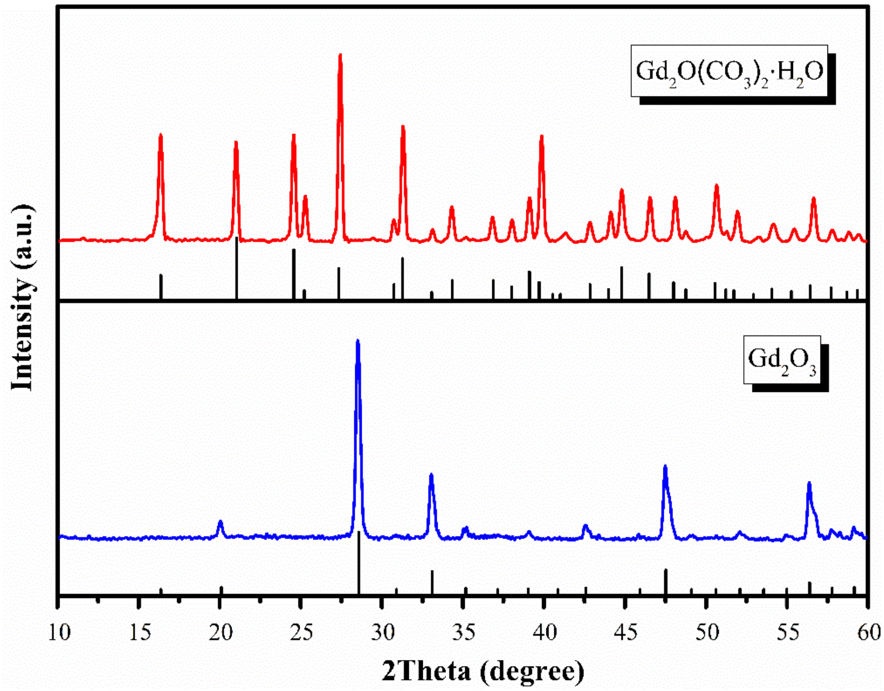

Figure S2. Typical XRD patterns of $Gd_2O(CO_3)_2 \cdot H_2O$:Yb^{3+},Er^{3+} and Gd_2O_3:Er^{3+},Yb^{3+} particles

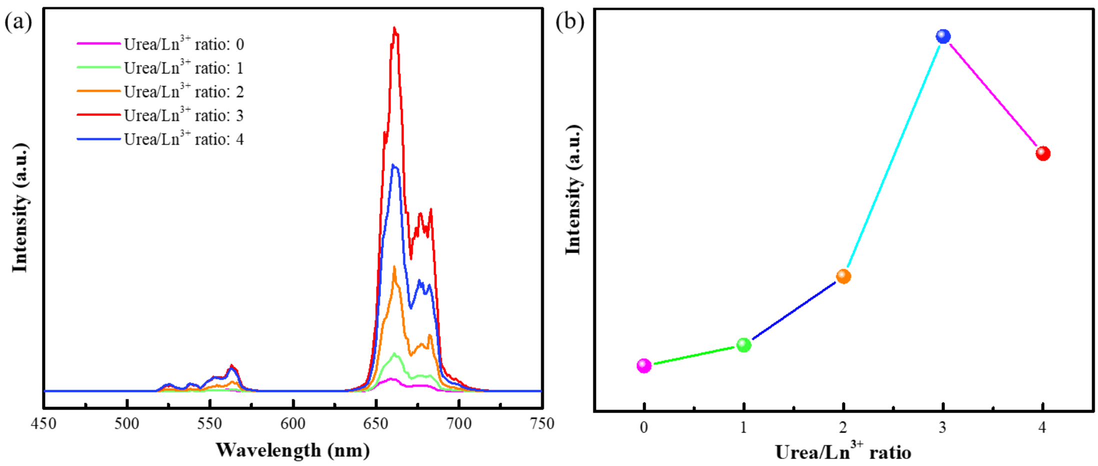

Figure S3. (a) Upconversion luminescence spectra of Gd_2O_3:10mol% Yb^{3+},1mol% Er^{3+} particles with different urea/Ln^{3+} ratio (b) The relationship between upconversion emission intensity and urea/Ln^{3+} ratios

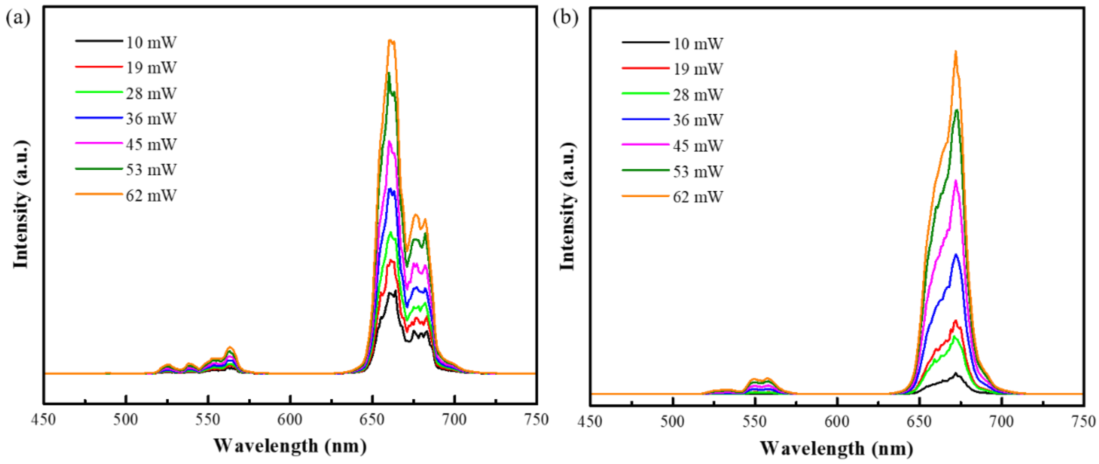

Figure S4. (a) Upconversion luminescence spectra of Gd_2O_3:10mol% Yb^{3+},1mol% Er^{3+} porous nanorods under different pump power. (b) Upconversion luminescence spectra of laser treated Gd_2O_3:10mol% Yb^{3+},1mol% Er^{3+} porous nanorods under different pump power.

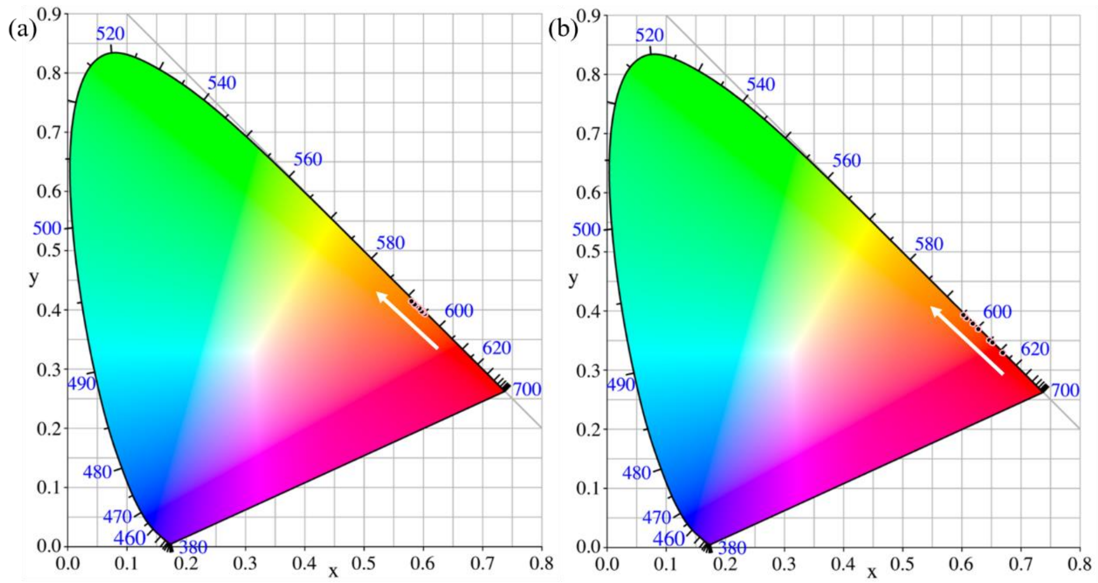

Figure S5. Power-dependence of the CIE coordinates (a) Gd_2O_3:10mol% Yb^{3+},1mol% Er^{3+} samples, (b) Gd_2O_3:10mol% Yb^{3+},1mol% Er^{3+} samples treated with 1.51W laser.

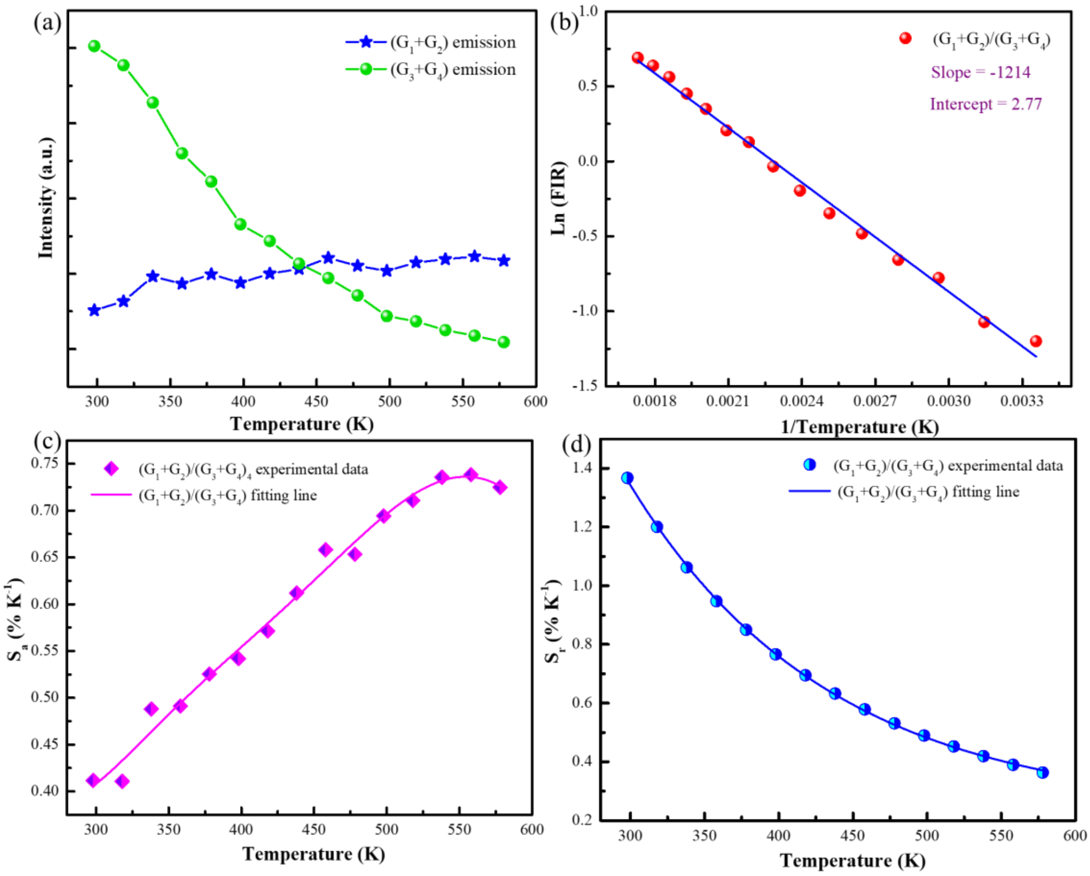

Figure S6. (a) Upconversion emission intensity varies the temperature of $^2H_{11/2} \rightarrow {}^4I_{15/2}$ and $^4S_{3/2} \rightarrow {}^4I_{15/2}$. (b) Monolog plot of the FIR from TCL pair ($^2H_{11/2}/^4S_{3/2}$) vs inverse absolute temperature. (c) Temperature dependence S_a of Gd_2O_3:10mol% Yb^{3+},1mol% Er^{3+} porous nanorods. (d) Temperature dependence S_r of Gd_2O_3:10mol% Yb^{3+},1mol% Er^{3+} porous nanorods.

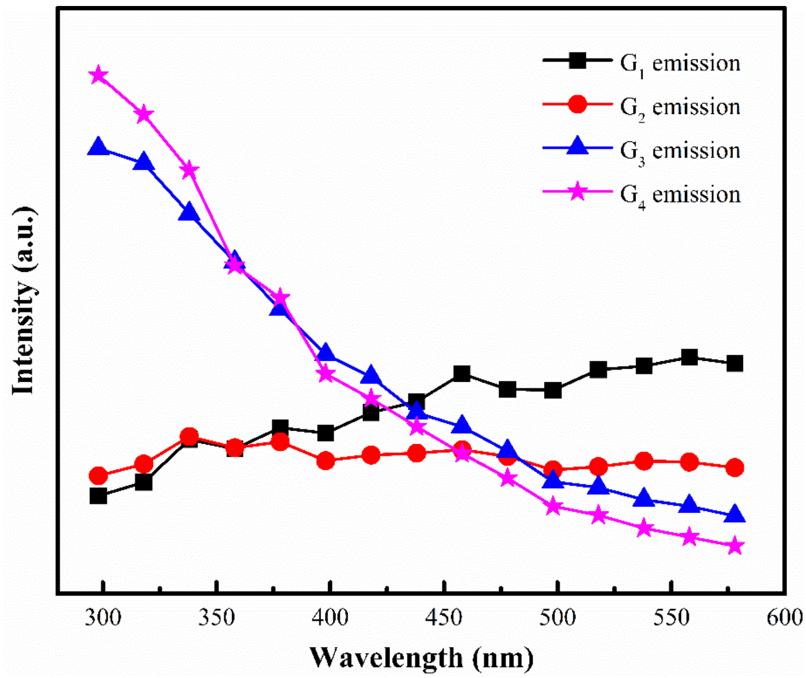

Figure S7. The luminescence intensity of stark sublevels G_1, G_2, G_3 and G_4 vs temperature for the Gd_2O_3:10mol% Yb^{3+},1mol% Er^{3+} porous nanorods.

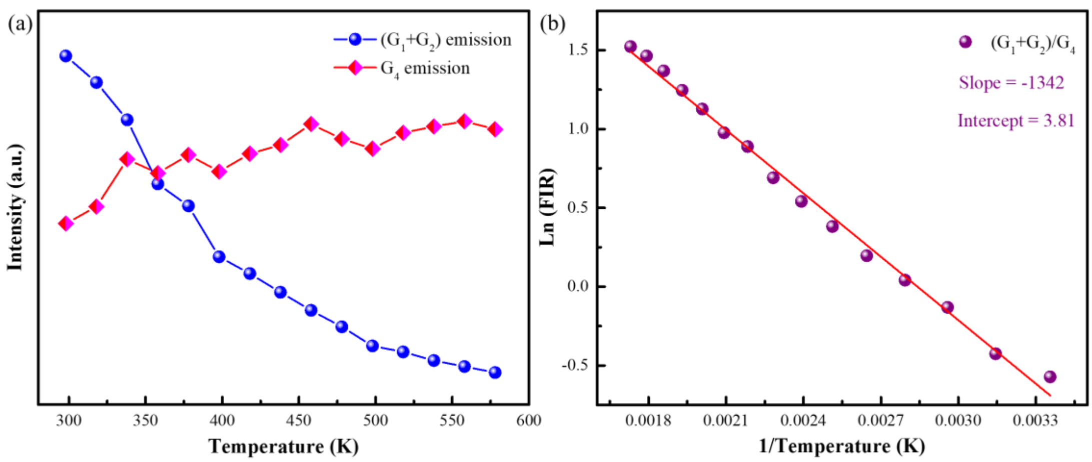

Figure S8. (a)The luminescence intensity of (G_1+G_2) and G_4 levels vs temperature for the Gd_2O_3:10mol% Yb^{3+},1mol% Er^{3+} porous nanorods. (b) Monolog plot of the FIR from TCL pair $(G_1+G_2)/G_4$ vs inverse absolute temperature.

Table S1. The Slope, Intercept and Fitting index (R^2) of linear fitting ($Ln(FIR_{HS}) = -\frac{\Delta E}{kT} + B$) for different TCL pairs.

TCLs	Slope	Intercept	Fitting index (R^2)
G_1/G_4	-1524	3.65	0.994
G_1/G_3	-1277	2.98	0.992
G_2/G_4	-1108	2.45	0.991
G_2/G_3	-889	1.84	0.994
$(G_1+G_2)/G_4$	-1214	2.77	0.994
$(G_1+G_2)/(G_3+G_4)$	-1342	3.81	0.994

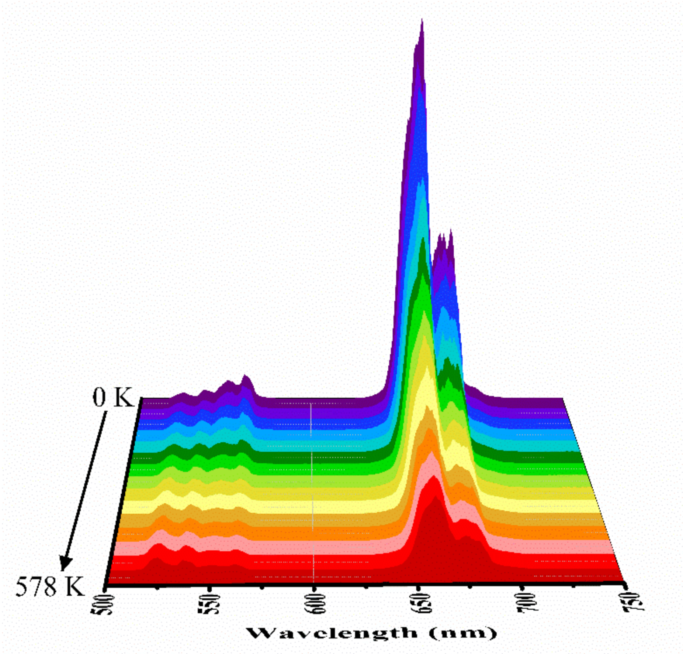

Figure S9. Upconversion emission spectra of Gd_2O_3:10mol% Yb^{3+},1mol% Er^{3+} under different temperature.